

Characterization of the Interface of Heterogeneous Blends of Polycarbonate and Polyfluorostyrene by  $^{13}\text{C}$ – $^{19}\text{F}$  REDOR NMRGang Tong<sup>†</sup> and Jacob Schaefer\*

Department of Chemistry, Washington University, St. Louis, Missouri 63130

Received May 6, 1997; Revised Manuscript Received August 7, 1997<sup>®</sup>

**ABSTRACT:** Blends of one part of carbonyl- $^{13}\text{C}$ , ring- $^{13}\text{C}$ , or methyl- $^{13}\text{C}$ -labeled polycarbonate with nine parts of poly(*p*-fluorostyrene) or poly(*o*-fluorostyrene) have been examined by  $^{13}\text{C}$ – $^{19}\text{F}$  rotational-echo double-resonance NMR. The immiscible blends were formed by precipitation from chloroform solution into methanol. After being annealed at 180 °C, the blends consist of domains of polycarbonate (average diameter of 36 nm) dispersed in a matrix of polyfluorostyrene. There are no kinetically trapped polycarbonate chains. The interface is tightly packed, with an average polycarbonate–polyfluorostyrene nearest-neighbor separation of labels of less than 4 Å. The interface is also partially ordered, with the  $^{19}\text{F}$  distances to the polycarbonate isopropylidene moiety greater than to the carbonate group. Despite the tight packing at the interface, polycarbonate ring dynamics in chains nearest to polyfluorostyrene are indistinguishable from those in bulk polycarbonate.

Most pairs of polymers are immiscible and form phase-separated, heterogeneous blends.<sup>1</sup> The commercially important properties of these blends depend on the structure and dynamics of chains at or near the phase boundaries.<sup>2</sup> Because these interfacial surfaces are not exposed, characterization of their structure and dynamics by conventional surface–science techniques is impractical.<sup>3</sup> If the domains are particularly small, or hard to contrast, scattering of X-rays or neutrons may not be options.<sup>4</sup> Finally, if both members of the pair have similar spin and molecular dynamics, there may be insufficient contrast for homonuclear NMR spin-diffusion measurements.<sup>5</sup> In this paper, we show that rotational-echo double-resonance<sup>6</sup> (REDOR)  $^{13}\text{C}$ – $^{19}\text{F}$  NMR can be used to determine domain size, interfacial packing, and interfacial chain dynamics in a heterogeneous blend of two completely amorphous polymers (one labeled by  $^{13}\text{C}$  and the other by  $^{19}\text{F}$ ) which have comparable NMR relaxation properties.

## Experimental Section

**Polymers.** The [carbonyl- $^{13}\text{C}$ ]polycarbonate was a kind gift from Eastman Kodak company. This polycarbonate had a weight-average molecular weight ( $M_w$ ) of 30 000 and a number-average molecular weight ( $M_n$ ) of 20 000, as measured by gel permeation chromatography. The [ring-3,3'- $^{13}\text{C}_2$ ]polycarbonate was synthesized by Dr. Stephen E. Bales of the Dow Chemical Company from labeled Bisphenol A purchased from Merck Stable Isotopes (formerly of Montreal, Canada). The ring-labeled polycarbonate was fractionated by partial precipitation using a 2:1 mixture of chloroform and methanol. The precipitated polycarbonate had a  $M_w$  of 33 000 and a  $M_n$  of 18 000. The [methyl- $^{13}\text{C}$ ]polycarbonate was synthesized by Jinhua Wu and Professor Albert F. Yee (University of Michigan) from labeled Bisphenol A also purchased from Merck Stable Isotopes. The resulting methyl-labeled polycarbonate had a  $M_w$  of 30 000 and a  $M_n$  of 20 000. All three labels were 99% at. %  $^{13}\text{C}$ .

Poly(*p*-fluorostyrene) and poly(*o*-fluorostyrene) were polymerized from monomers purchased from Monomer-Polymers Laboratories, Inc. by heating to 70 °C for 24 h, followed by a gradual increase of the temperature to 120 °C at a rate of 10 °C per day. Both polymers had an  $M_w$  of 240 000 and an  $M_n$  of 120 000.

Blends of polycarbonate and polyfluorostyrene were prepared by first dissolving<sup>7</sup> the two polymers in the common solvent chloroform at a total concentration of 1 g/100 mL. This solution was then precipitated either dropwise into a large excess of methanol or batchwise using a volume of methanol about 4 times that of the chloroform solution. The fine precipitant was washed several times with methanol, air-dried overnight, vacuum-dried at room temperature for 2 days, and finally vacuum-dried at 70 °C for 5 h. All blends were 19% (by weight) polycarbonate (0.1 mol fraction).

**NMR Spectrometer.** Cross-polarization, magic-angle spinning, Hahn-echo  $^{13}\text{C}$  NMR spectra were obtained at room temperature using a superconducting solenoid operating at 4.7 T. The single, 9-mm diameter, radio-frequency coil was connected by a low-loss transmission line<sup>8</sup> to a quadruple-resonance tuning circuit,<sup>9</sup> which permits  $^1\text{H}$ ,  $^{19}\text{F}$ ,  $^{13}\text{C}$ , and  $^{15}\text{N}$  detection or dephasing at 200, 188, 50, and 20 MHz, respectively. In these experiments, the  $^{15}\text{N}$  channel was not used. Proton–carbon cross-polarization transfers were performed in 2 ms at 50 kHz, followed by proton and fluorine dipolar decoupling at 90 kHz. Fluorine–carbon cross-polarization transfers were also made in 2 ms under a one-spinning speed Hartmann–Hahn frequency mismatch<sup>10</sup> ( $^{19}\text{F}$  and  $^{13}\text{C}$  radio-frequency field amplitudes of 45 and 50 kHz, respectively) and active control ( $\pm 200$  Hz) of the applied fields. The magic-angle stators were obtained from Chemagnetics (Fort Collins, CO). High-performance 7.5-mm o.d. zirconia rotors were fitted with boron nitride spacers and plastic (Kel-F) end and drive caps and supported at both ends by air-pumped journal bearings.

**REDOR.** The pulse sequence used for rotational-echo, double-resonance (REDOR) experiments<sup>6</sup> is illustrated in Figure 1 (first half of each sequence). The single  $^{13}\text{C}$   $\pi$  pulse in the middle of the REDOR carbon-magnetization dephasing period (top left) refocuses all isotropic chemical shifts at the start of data acquisition. In the absence of any  $^{19}\text{F}$  pulses, a Fourier transform of the echo that forms results in  $S_0$ , the REDOR full-echo spectrum, which, for this sequence, is also the CPMAS Hahn-echo spectrum. Application of XY phase-alternated<sup>11</sup> fluorine  $\pi$  pulses every half rotor cycle causes a net dephasing of the transverse magnetization of those carbons dipolar coupled to  $^{19}\text{F}$ . The resulting spectrum,  $S$ , is diminished in intensity. The REDOR difference spectrum ( $\Delta S = S_0 - S$ ) arises only from those carbons that are dipolar coupled to fluorine. REDOR dephasing was accumulated over 4–160 rotor cycles, with magic-angle spinning at 5 kHz. Because sidebands dephase at a rate different from centerbands,<sup>6</sup> residual spinning sidebands should not be suppressed in REDOR experiments.

**DRAMA.** Dipolar restoration at the magic angle<sup>12</sup> (DRAMA) uses rotor-synchronized 90° pulses to dephase the magnetiza-

<sup>†</sup> Present address: Department of Biochemistry, Duke University Medical Center, Durham, NC 27710.

<sup>®</sup> Abstract published in *Advance ACS Abstracts*, October 15, 1997.

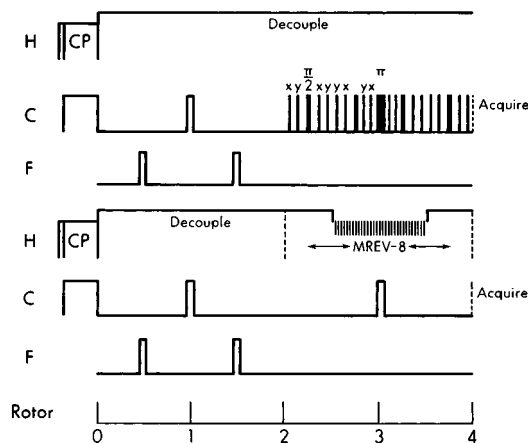


**Figure 1.** Pulse sequences for rotational-echo double resonance (REDOR) combined with dipolar restoration at the magic angle (DRAMA, second half of top sequence), or dipolar rotational spin echo NMR (DRSE, second half of bottom sequence). Both illustrations are for four rotor cycles.

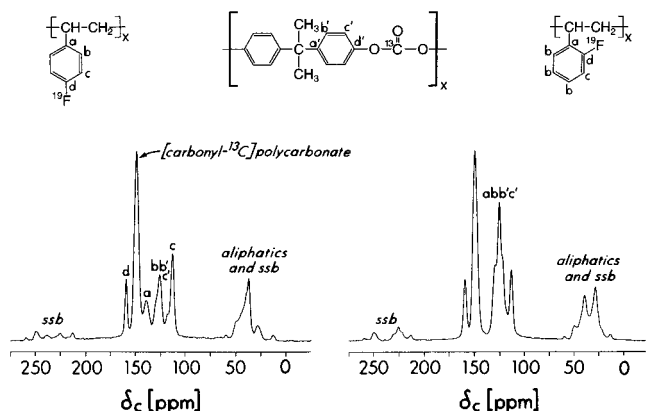


**Figure 2.** Cross-polarization magic-angle spinning  $^{13}\text{C}$  NMR spectra of immiscible blends of [carbonyl- $^{13}\text{C}$ ]polycarbonate with poly(*p*-fluorostyrene) (left) or poly(*o*-fluorostyrene) (right). Both blends were formed by dropwise precipitation from a chloroform solution into methanol. The blends were not annealed. The spectra were obtained with 5-kHz magic-angle spinning and both proton and fluorine dipolar decoupling at 90 kHz.

tion of isolated homonuclear pairs of dipolar-coupled spin  $1/2$  nuclei. The full XY8-DRAMA sequence<sup>13</sup> is shown in Figure 1 (top, right). The  $\pi$  pulses at the completion of the odd-numbered rotor cycles refocus isotropic chemical shifts at the completion of the even-numbered rotor cycles. These  $\pi$  pulses are phase alternated following the XY8 scheme<sup>11</sup> (xyxyxyxy). A complete phase cycle therefore requires 16 rotor cycles. The phase of the leading pulse of the XY8 sequence is determined by the  $^{13}\text{C}$ -spin quadrature routing.

The frequency-offset dependence of DRAMA due to chemical-shift tensors (and 1–2 kHz isotropic chemical-shift differences) is removed using eight equally spaced  $\pi$  pulses per rotor cycle.<sup>13</sup> These pulses are placed at  $1/16, 3/16, 5/16, \dots$  of the rotor period ( $T_r$ ). The phases of these  $\pi$  pulses are also alternated according to the XY8 scheme. Phase accumulation at the spinning frequency and twice the spinning frequency from chemical-shift interactions for transverse magnetization arising from individual crystallites in an isotropic powder cancel under the four sign reversals created in each half rotor cycle by the eight  $\pi$  pulses.<sup>13</sup> Two  $90^\circ$  pulses per rotor period are placed at  $1/4 T_r$  and  $3/4 T_r$  for maximum dephasing. These pulses all have the same phase which is determined by the  $^{13}\text{C}$  quadrature routing. The signal that forms at the completion of even numbers of rotor cycles using the sequence of Figure 1 (top, right) is called the DRAMA-dephased echo,  $S$ . In the absence of the  $^{13}\text{C}$   $\pi/2$  pulses, the signal that forms at the completion of even numbers of rotor cycles is the DRAMA full

### Polycarbonate / Poly(*p*-fluorostyrene)

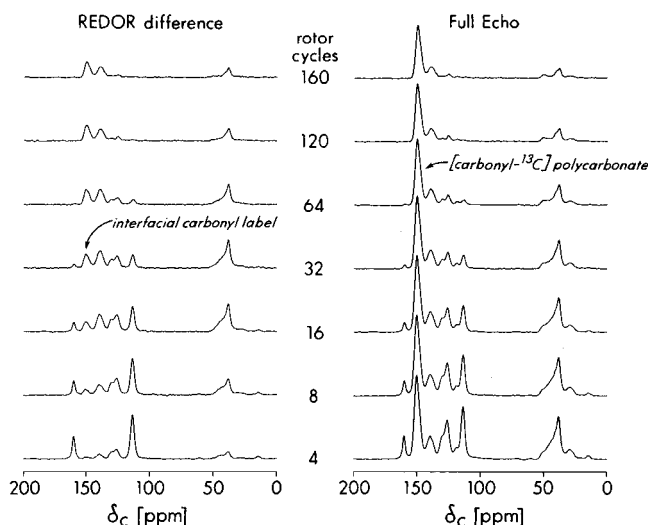


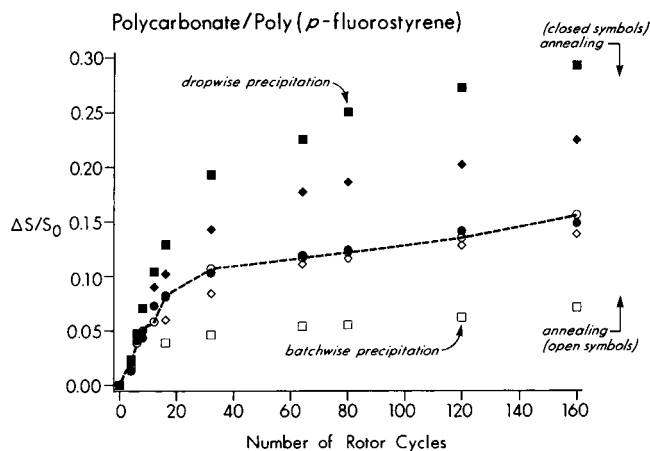
**Figure 3.** REDOR  $^{13}\text{C}$  NMR spectra (with  $^{19}\text{F}$  dephasing) for the polycarbonate–poly(*p*-fluorostyrene) blend of Figure 2 (left). The spectra were obtained with 5-kHz magic-angle spinning and 90-kHz proton dipolar decoupling.

echo,  $S_0$ . The  $^{13}\text{C}$  DRAMA difference is  $\Delta S = S_0 - S$ . DRAMA was calibrated for  $^{13}\text{C}$ – $^{13}\text{C}$  distance determinations by measurement of the known two-bond distance in [1,3- $^{13}\text{C}_2$ ,  $^{15}\text{N}$ ]alanine. The combination REDOR–DRAMA experiment uses a double difference in which four kinds of spectra were obtained: with and without REDOR dephasing and each with and without DRAMA dephasing. Magic-angle spinning was at 5 kHz.

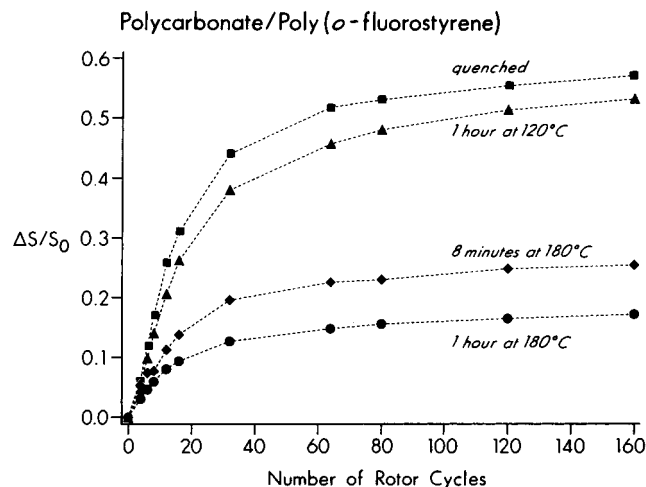
**DRSE.** Carbon dipolar line shapes were characterized by a version of dipolar rotational spin-echo (DRSE)  $^{13}\text{C}$  NMR extended over two rotor cycles.<sup>14</sup> This is a two-dimensional experiment in which, during the additional time dimension, carbon magnetization is allowed to evolve under the influence of  $^1\text{H}$ – $^{13}\text{C}$  coupling while  $^1\text{H}$ – $^1\text{H}$  coupling is suppressed by homonuclear multiple-pulse semiwindowless MREV-8 decoupling<sup>15</sup> (Figure 1, bottom right). The cycle time for the homonuclear decoupling pulse sequence was 33.6  $\mu\text{s}$ , resulting in decoupling of proton–proton interactions as large as 60 kHz. Sixteen MREV-8 cycles fit exactly into two rotor periods with magic-angle spinning at 3720 Hz. REDOR-selected DRSE time evolution was obtained by the difference of DRSE dipolar evolution preceded by 16 rotor cycles of REDOR, once with  $^{19}\text{F}$   $\pi$  pulses (Figure 1, bottom) and once without  $^{19}\text{F}$   $\pi$  pulses.

## Results

**Annealing and REDOR Dephasing.** The  $^{13}\text{C}$  NMR spectra of [carbonyl- $^{13}\text{C}$ ]polycarbonate blended with either poly(*p*-fluorostyrene) or poly(*o*-fluorostyrene) have major peaks from the  $^{13}\text{C}$  label whose resonance occurs at 150 ppm (Figure 2). Natural-abundance peaks for the nonprotonated ring carbons of polycarbonate also occur at this shift position,<sup>16</sup> but even combined are 25 times less intense. For the blend of [carbonyl- $^{13}\text{C}$ ]polycarbonate with poly(*p*-fluorostyrene) formed by dropwise precipitation, a REDOR difference peak appears at 150 ppm after only four rotor cycles of  $^{19}\text{F}$  dephasing (Figure 3, bottom, left). The 150-ppm difference peak is the largest in the REDOR difference spectrum after 160 rotor cycles of dephasing (Figure 3, top, left) and corresponds to a  $\Delta S/S_0$  of nearly 30%. The observed dephasing decreases to about 15% after annealing at a temperature greater than the  $T_g$  of polycarbonate (Figure 4, solid symbols). The corresponding blend formed by batchwise precipitation has a  $\Delta S/S_0$  at 150 ppm of only 7% after 160 rotor cycles, but the



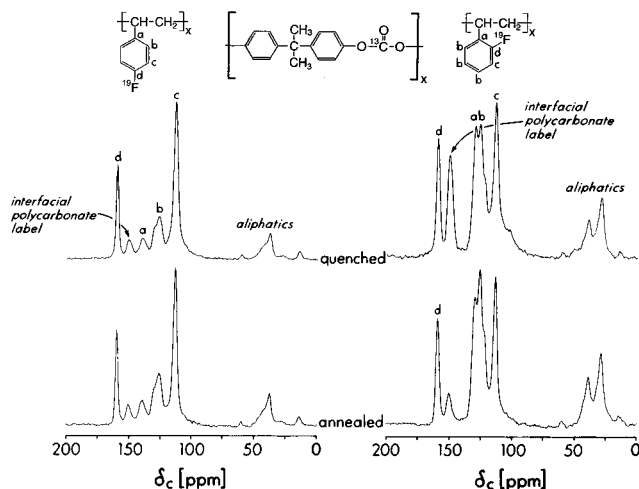
**Figure 4.** REDOR dephasing ( $\Delta S/S_0$ ) of the 150-ppm peak for the polycarbonate–poly(*p*-fluorostyrene) blend of Figure 2 (left) after no annealing (solid squares), annealing for 1 h at 145 °C (solid diamonds), and annealing for 1 h at 180 °C (solid circles). The open symbols show the corresponding REDOR dephasing for an immiscible blend of [carbonyl- $^{13}\text{C}$ ]polycarbonate with poly(*p*-fluorostyrene) formed by batchwise precipitation after no annealing (open squares), annealing for 1 h at 160 °C (open diamonds), and annealing for one hour at 180 °C (open circles). Magic-angle spinning was at 5 kHz.



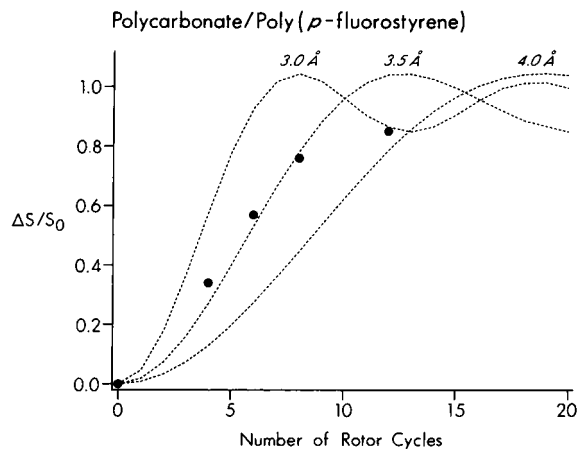
**Figure 5.** REDOR dephasing ( $\Delta S/S_0$ ) of the 150-ppm peak for the polycarbonate–poly(*o*-fluorostyrene) blend of Figure 2 (right) after no annealing (solid squares), annealing for 1 h at 120 °C (solid triangles), annealing for 8 min at 180 °C (solid diamonds), and annealing for 1 h at 180 °C (solid circles). Magic-angle spinning was at 5 kHz.

observed dephasing increases with annealing and also reaches a final value of about 15% (Figure 4, open symbols). The dephasing behavior at 150 ppm on annealing for the blend of [carbonyl- $^{13}\text{C}$ ]polycarbonate with poly(*o*-fluorostyrene) formed by dropwise precipitation is similar to that of the dropwise precipitated blend with poly(*p*-fluorostyrene), but with  $\Delta S/S_0$  of 57% before annealing and 17% after annealing (Figure 5).

**Fluorine–Carbon Cross-Polarization Preparation for REDOR Dephasing.** Cross-polarization transfer from one rare spin to another is sensitive to the Hartmann–Hahn match.<sup>17</sup> We observed essentially no transfer when the match offset was zero and a maximum transfer when the offset was exactly one spinning speed.<sup>10,17</sup> The observed ratios of intensities of polyfluorostyrene aromatic-ring carbon peaks identified as “c” (two bonds from  $^{19}\text{F}$ ) and “d” (one bond from  $^{19}\text{F}$ ) are the same regardless of whether the cross-polarization transfers were from protons (Figure 2) or from fluorines

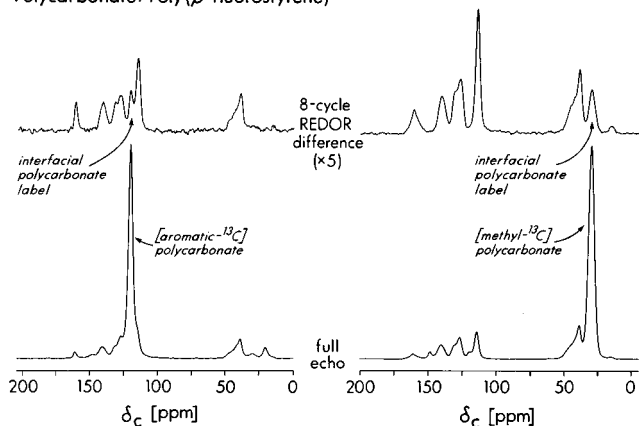


**Figure 6.** Fluorine-to-carbon cross-polarization magic-angle spinning  $^{13}\text{C}$  NMR spectra of immiscible blends of [carbonyl- $^{13}\text{C}$ ]polycarbonate with poly(*p*-fluorostyrene) formed by batchwise precipitation (left) and poly(*o*-fluorostyrene) formed by dropwise precipitation (right). Spectra of the blends before annealing are shown at the top of the figure and after annealing for 1 h at 180 °C at the bottom of the figure. The spectra were obtained with 5-kHz magic-angle spinning and both proton and fluorine dipolar decoupling at 90 kHz.

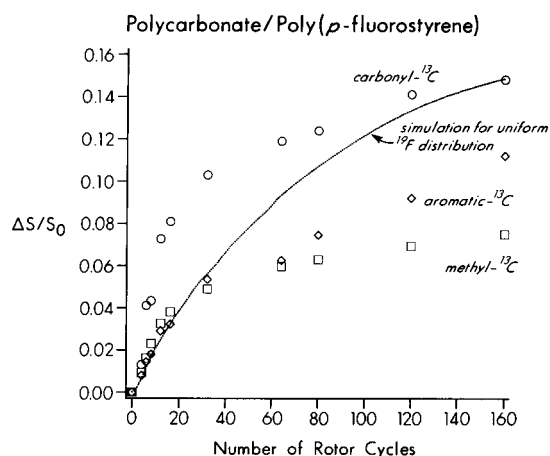


**Figure 7.** REDOR dephasing ( $\Delta S/S_0$ ) of the  $^{19}\text{F} \rightarrow ^{13}\text{C}$  150-ppm peak for the [carbonyl- $^{13}\text{C}$ ]polycarbonate–poly(*p*-fluorostyrene) blend of Figure 6 (bottom left). The dotted lines were calculated assuming an isolated  $^{13}\text{C}$ – $^{19}\text{F}$  spin pair.

(Figure 6), assuming that the latter have been optimized. The  $^{19}\text{F} \rightarrow ^{13}\text{C}$  150-ppm signal intensity from [carbonyl- $^{13}\text{C}$ ]polycarbonate in the blend with poly(*p*-fluorostyrene) formed by batchwise precipitation is insensitive to annealing (Figure 6, left), whereas the corresponding signal from labeled polycarbonate in the blend with poly(*o*-fluorostyrene) formed by dropwise precipitation decreases in intensity by a factor of 4 on annealing (Figure 6, right). The  $^{19}\text{F} \rightarrow ^{13}\text{C}$  150-ppm  $^{13}\text{C}$  signal in the annealed blend with poly(*p*-fluorostyrene) is comparable in absolute intensity to that of the REDOR  $\Delta S$  ( $N_c = 12$ ) for the same blend and, in fact, undergoes almost 90% REDOR dephasing by  $^{19}\text{F}$  in only 12 rotor periods (Figure 7, solid circles). The  $^{19}\text{F} \rightarrow ^{13}\text{C}$  transfer depends on the inverse sixth power of the internuclear separation<sup>10</sup> and is therefore a short-range process. The equivalence of intensities between  $^{19}\text{F} \rightarrow ^{13}\text{C}$  transfers and REDOR dephasing after just a few rotor periods proves that the first REDOR difference signal to appear is due to a few polycarbonate chains near the interface, rather than to many polycarbonate chains farther away.

Polycarbonate/Poly(*p*-fluorostyrene)

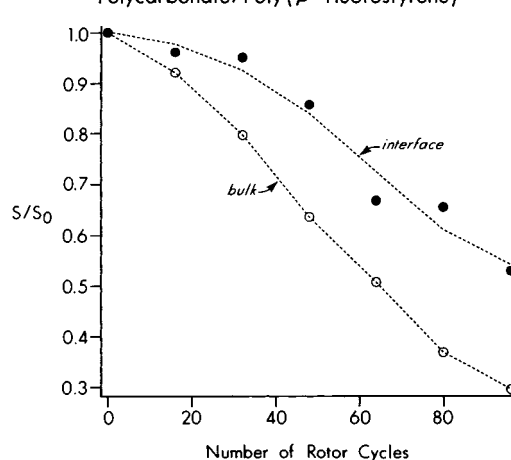
**Figure 8.** REDOR  $^{13}\text{C}$  NMR spectra of immiscible blends of poly(*p*-fluorostyrene) with [ring- $^{13}\text{C}$ ]polycarbonate (left) or [methyl- $^{13}\text{C}$ ]polycarbonate (right) formed by dropwise precipitation. The spectra were obtained with 5-kHz magic-angle spinning and 90-kHz dipolar decoupling.



**Figure 9.** REDOR dephasing ( $\Delta S/S_0$ ) for the  $^{13}\text{C}$  NMR peaks at 150 ppm (circles, carbonate- $^{13}\text{C}$ ), 120 ppm (diamonds, ring- $^{13}\text{C}$ ), and 30 ppm (squares, methyl- $^{13}\text{C}$ ) of immiscible blends of three labeled polycarbonates with poly(*p*-fluorostyrene), each formed by dropwise precipitation and annealed for 1 h at 180 °C. The dotted line is the calculated multispin dephasing expected for uniform interfacial distributions of  $^{19}\text{F}$  and  $^{13}\text{C}$  labels. See text for details.

**Position of the Carbon Label in Polycarbonate and REDOR Dephasing.** REDOR  $^{13}\text{C}$  NMR spectra of [ring- $^{13}\text{C}$ ]polycarbonate, and of [methyl- $^{13}\text{C}$ ]polycarbonate, each in an unannealed blend with poly(*p*-fluorostyrene) formed by dropwise precipitation, are shown in Figure 8. The full-echo 120-ppm aromatic-carbon signal and the 30-ppm methyl-carbon are both resolved; the REDOR difference peaks (after eight rotor cycles of dephasing) at these frequencies therefore arise exclusively from polycarbonate chains at or near the interface (see above). The total REDOR dephasing after 160 rotor cycles for the aromatic-carbon label is greater than that of the methyl-carbon label, but less than that of the carbonyl-carbon label (Figure 9).

**REDOR Dephasing as Preparation for DRAMA and DRSE.** Each of the combination experiments<sup>18</sup> whose pulse sequences are illustrated in Figure 1 use REDOR dephasing to select signals from  $^{13}\text{C}$ -labeled polycarbonate chains at the interface for structural (DRAMA) or dynamical (DRSE) characterization. REDOR preparation of 16 rotor cycles of  $^{19}\text{F}$  dephasing selects only those polycarbonate chains that are nearest the interface. (We ignore contributions to the spectra

Polycarbonate/Poly(*p*-fluorostyrene)

**Figure 10.** DRAMA dephasing ( $\Delta S/S_0$ ) of the 150-ppm line of the immiscible blend of [carbonyl- $^{13}\text{C}$ ]polycarbonate with poly(*p*-fluorostyrene) formed by dropwise precipitation after annealing for 1 h at 180 °C. The pulse sequence of Figure 1 (top) was used with and without REDOR dephasing, and with and without DRAMA dephasing. Double differences separated bulk and interfacial signals. Magic-angle spinning was at 5 kHz.

from polyfluorostyrene, which are distinguishable by their chemical shifts.) For example, without REDOR dephasing by  $^{19}\text{F}$  preceding DRAMA, the REDOR-DRAMA experiment of Figure 1 is the same as regular DRAMA and results in a full-echo  $S_0$ , and DRAMA-dephased echo  $S$ , for the entire sample (bulk plus interface). With  $^{19}\text{F}$  dephasing pulses, however, the interfacial signal is dephased before the application of the DRAMA pulses. The DRAMA spectra of polycarbonate in the bulk are then obtained. The differences between with and without the  $^{19}\text{F}$  dephasing are then the DRAMA spectra of polycarbonate chains at the interface. As shown in Figure 10 for the annealed blend of [carbonyl- $^{13}\text{C}$ ]polycarbonate with poly(*p*-fluorostyrene), the DRAMA dephasing for the  $^{13}\text{C}$  label at the interface is less than that for the  $^{13}\text{C}$  label in the bulk.

The REDOR-DRSE combination experiment involves a similar differencing procedure to separate bulk and interfacial signals. The DRSE dephasing for the 120-ppm signal from bulk [aromatic- $^{13}\text{C}$ ]polycarbonate is zero after four MREV-8 cycles (Figure 11, left), and so is that for interfacial polycarbonate (Figure 11, right). Both patterns are characteristic of phenylene rings undergoing large-amplitude motions that reduce  $^1\text{H}$ - $^{13}\text{C}$  dipolar couplings.<sup>16</sup> By way of contrast, the DRSE dephasing for aromatic-carbon line c of the polyfluorostyrene is zero after only two MREV-8 cycles (Figure 11, right).

## Discussion

**Annealing.** We envision dropwise precipitation of polycarbonate-polyfluorostyrene blends as a fast process during which a local excess of nonsolvent methanol displaces chloroform quickly enough that some polycarbonate chains do not have time to escape the proximity of polyfluorostyrene chains before aggregation occurs. These trapped polycarbonate chains might exist alone or in small bundles with a high ratio of surface area to volume. The net result for the labeled blends is many contacts between  $^{13}\text{C}$  and  $^{19}\text{F}$  labels and consequently a large  $\Delta S/S_0$  (Figure 4). Annealing at 180 °C allows smaller domains to merge with each other or with larger domains with which there is already contact. This

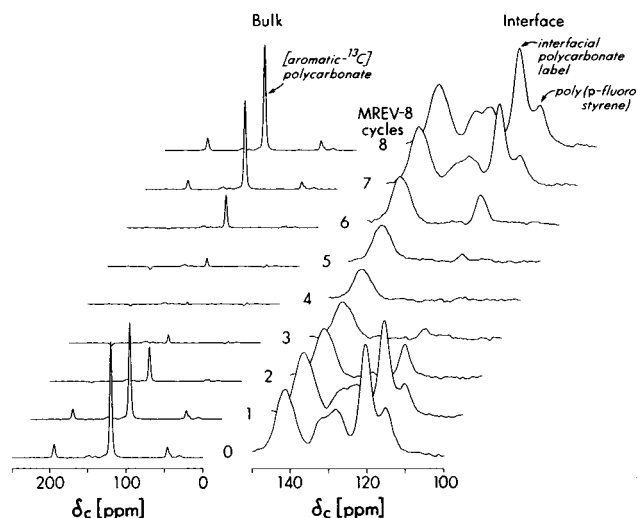


**Figure 11.** DRSE  $^{13}\text{C}$  NMR spectra of the immiscible blend of [ring  $^{13}\text{C}$ ]polycarbonate with poly(*p*-fluorostyrene) formed by dropwise precipitation after annealing for 1 h at 180 °C. The pulse sequence of Figure 1 (bottom) was used with and without  $^{13}\text{C}$ – $^{19}\text{F}$  REDOR dephasing (to separate bulk and interfacial signals; see text), and with and without MREV-8 scaled  $^1\text{H}$ – $^{13}\text{C}$  dephasing. The spectra were obtained using 3720-Hz magic-angle spinning and 90-kHz proton dipolar decoupling.

results in a corresponding decrease in the observed REDOR dephasing. Further consolidation into macroscopic domains apparently does not occur, at least under the annealing conditions of these experiments, because sizeable REDOR dephasing persists.

Batchwise precipitation, on the other hand, is apparently a much slower process, with time for most polycarbonate chains to find polycarbonate neighbors as methanol and chloroform exchange. The net result is few contacts between  $^{13}\text{C}$  and  $^{19}\text{F}$  labels and a small  $\Delta S/S_0$ . For these precipitates, REDOR dephasing increases with annealing, presumably because of the densification in packing of next-nearest layers of polycarbonate chains relative to the boundary defined by the nearest polyfluorostyrene chain. The insensitivity of the intensity of the  $^{19}\text{F} \rightarrow ^{13}\text{C}$  150-ppm peak to 180 °C annealing (Figure 6, left) shows that nearest neighbors to the interfacial boundary are established in batchwise precipitation. We take this result to mean that there are no gaps between polycarbonate and polyfluorostyrene domains in quenched blends that must be filled in by annealing.

**Polycarbonate First Layer.** The  $^{19}\text{F} \rightarrow ^{13}\text{C}$  150-ppm peak represents about one-third to one-half of the REDOR  $\Delta S$  after 160 rotor cycles of dephasing. As mentioned before, the  $^{19}\text{F} \rightarrow ^{13}\text{C}$  peak necessarily arises from polycarbonate–polyfluorostyrene nearest neighbors because of the short-range nature of a cross-polarization transfer between two rare-spin systems.<sup>10,17</sup> Translation of a cross-polarization transfer rate into a distance is a difficult calculation,<sup>10</sup> which requires detailed knowledge of the local  $^{19}\text{F}$ – $^{19}\text{F}$  dipolar coupling. Although we know that the average bulk  $^{19}\text{F}$ – $^{19}\text{F}$  coupling is about 500 Hz from spin echo  $T_2$  experiments (data not shown), and the interfacial value is likely to be similar, we have not actually measured the homonuclear coupling at the interface (for example, by a REDOR-selected  $^{19}\text{F}$   $T_2$ ). Nevertheless, we are able to make a quantitative estimate of the average separation of nearest-neighbor polycarbonate–polyfluorostyrene by

REDOR dephasing of the signal selected by the  $^{19}\text{F} \rightarrow ^{13}\text{C}$  transfer. This dephasing (Figure 7) suggests<sup>19</sup> a modest distribution of distances for the nearest-neighbor  $^{19}\text{F}$ – $^{13}\text{C}$  isolated pair (the  $^{19}\text{F}$  concentration is too low for significant numbers of clusters of fluorines) centered about 3.5 Å. We estimate the distribution of spacings as about  $\pm 15\%$  of the average internuclear separation.

**Domain Size.** If we assume that after annealing at 180 °C the polycarbonate domains are spherical droplets in a polyfluorostyrene matrix, then the observed  $\Delta S/S_0$  is determined by the fraction of polycarbonate chains at or near the interface relative to the fraction in the bulk. That is,  $\Delta S/S_0 = (4\pi R^2 L)/(4\pi R^3/3)$ , where  $R$  is the radius of the polycarbonate domain and  $L$  is the thickness of the interface. We define  $L$  in terms of the effective dephasing range of  $^{19}\text{F}$ – $^{13}\text{C}$  REDOR for 160 rotor cycles and 5-kHz magic-angle spinning. This distance is about 12 Å, so  $L$  is 9 Å (the dephasing range minus the shortest  $^{13}\text{C}$ – $^{19}\text{F}$  distance of Figure 7 of 3 Å). For an observed REDOR dephasing of 15% (Figures 4 and 5),  $R \approx 180$  Å. REDOR determines an average value of  $R$  but provides no insight into the distribution of domain sizes. The estimate for  $R$  would increase if we were to take into account any bumps<sup>20</sup> on the surface of the polycarbonate spheres which would increase  $^{13}\text{C}$ – $^{19}\text{F}$  contact, assuming that the polyfluorostyrene phase conformed to the shape of the polycarbonate bumps.

**Local Ordering.** Experimental<sup>19</sup> and theoretical<sup>21</sup> analysis of the packing of polycarbonate chains suggest an interchain spacing of about 6 Å. Assuming similar packing in the blends, only two layers of polycarbonate are within the 12-Å  $^{19}\text{F}$ – $^{13}\text{C}$  dephasing range: the nearest-neighbor layer (3–4 Å away from the interfacial boundary) and the next-nearest neighbor layer (about 10 Å away).

We have shown<sup>19</sup> that local orientational order exists in bulk polycarbonate. To determine whether packing of polycarbonate chains at the interface also has elements of orientational order, we need to translate the REDOR dephasing of Figure 9 into at least semiquantitative average distances of  $^{19}\text{F}$  to carbonate-, ring-, and methyl-carbon  $^{13}\text{C}$  positions of polycarbonate. This requires specifying the positions of all fluorine dephasing centers within 12 Å of a given  $^{13}\text{C}$  label. We assume a uniform cubic array of  $^{19}\text{F}$  positions with a  $^{19}\text{F}$ – $^{19}\text{F}$  separation of 6 Å. This value is estimated from the average  $^{19}\text{F}$ – $^{19}\text{F}$  dipolar coupling at the interface which we take as 500 Hz. We make no distinction between poly(*p*-fluorostyrene) and poly(*o*-fluorostyrene), which seem to behave similarly (Figures 4 and 5). We adopt a coordinate system centered on one fluorine at the interface so that we can specify a nearby interfacial fluorine by, for example, (6,0,0) and another by (0,6,0), and so on. We will average polycarbonate positions over just three types of configurations: (0,0, $z$ ), (3,0, $z$ ), and (3,3, $z$ ), where  $z$  is 3 Å for  $^{13}\text{C}$ – $^{19}\text{F}$  nearest-neighbors, and 9 Å for next-nearest neighbors. These three positions represent  $^{13}\text{C}$  labels opposite the corner of a  $^{19}\text{F}$  cube, the middle of an edge of the cube, and the middle of a face. For a  $^{13}\text{C}$  at (0,0,3), there is an array of 18 fluorines within 12 Å, but the dephasing is dominated by the single  $^{19}\text{F}$  which is 3 Å away. For other configurations, more of the  $^{19}\text{F}$  centers make important contributions to the dephasing.

Dephasing from many  $^{19}\text{F}$  spins is taken into account<sup>22</sup> by a powder average of a sum of independent

dephasings, which equals the powder average of the product of those dephasings:  $S/S_0 = \langle \cos(\sum \phi_{Di}) \rangle_{\text{space and spin}} = \langle \Pi \cos(\phi_{Di}) \rangle_{\text{space}}$ , where  $\phi_{Di}$  is the phase accumulation<sup>6</sup> resulting from the dipolar coupling between a  $^{13}\text{C}$  label and the  $i$ th  $^{19}\text{F}$  atom. The first angle bracket indicates an average over space and spin coordinates, and the second angle bracket indicates just a spatial powder average. The spatial average requires the use of three Euler angles.<sup>23</sup> The average over spin coordinates includes dephasing by  $^{19}\text{F}$ – $^{13}\text{C}$  pairs that have parallel spins (positive  $\phi_D$ ) and antiparallel spins (negative  $\phi_D$ ) and takes advantage of the additivity of arguments for the products of exponentials.<sup>23</sup> This is a standard averaging procedure in SEDOR calculations for multiple dephasing spins.<sup>24</sup>

The dotted line in Figure 9 shows the calculated REDOR dephasing if the carbon labels are distributed uniformly; that is, the positions of a given type of label are represented by an equal-weight, three-fold average (corner, center edge, and center face) over the assumed cubic array of fluorine dephasing centers described above. The calculated  $\Delta S/S_0$  has been scaled to 0.15 for  $N_C = 160$ . The experimental initial dephasing for the carbonate- $^{13}\text{C}$  label clearly exceeds the calculated values, which suggests an orientational preference, perhaps the result of electrostatic attractions between electronegative fluorines and electron-density depleted carbons. This is consistent with the tight packing demanded by the 3.5-Å separation of  $^{19}\text{F}$  and carbonate- $^{13}\text{C}$  from Figure 7. Although the initial dephasing for aromatic- and methyl- $^{13}\text{C}$  labels matches the calculated values, the dephasing for  $N_C > 40$  does not, so orientational preferences apparently also extend to chains that are more distant from the interface than the nearest neighbors. We conclude that polycarbonate chain packing at the interface has local orientational order with respect to the neighboring polyfluorostyrene chains. A more quantitative conclusion requires additional labeling experiments in combination with molecular modeling.

None of the calculations used for Figure 9 took motion into account. Large-amplitude motions are not present for carbonate-<sup>25</sup> or methyl-carbons<sup>26</sup> but are a possibility for the phenylene rings.<sup>27,28</sup> Determinations of ring orientations relative to the interface are well beyond the scope of this work. However, we believe that ignoring ring motions like flips in the simulations is acceptable because these motions have little averaging effect on dipolar couplings to distant  $^{19}\text{F}$  dephasing centers.<sup>29</sup> We consider the question of whether the rings in polycarbonate chains at the interface are actually flipping in the next section.

**Polycarbonate Ring Dynamics.** A point-for-point comparison of the time-domain results of Figure 11 for bulk and interfacial ring  $^{13}\text{C}$  polycarbonate shows that the two types of chains are indistinguishable by DRSE. Thus, polycarbonate rings at the interface are flipping.<sup>16</sup> The Whitney–Yaris model<sup>21</sup> for ring flips in polycarbonate has two essential elements: (i) each polycarbonate repeat unit is six coordinate, with two intrachain and four interchain nearest neighbors and (ii) the ring-flip gate is provided by the dynamics of just one of the interchain nearest neighbors. For the polycarbonate chain in the blend nearest the interface, one of the interchain nearest neighbors is an immobile polyfluorostyrene ring less than 4 Å away. Thus, the remaining polycarbonate interchain nearest neighbor must be the gate. The packing orientation for the gate places an isopropylidene of one chain of the pair opposite

a carbonate of the other. The remaining two interchain nearest neighbors for a polycarbonate chain closest to the interface are therefore packed with all three carbonates lined up (see Figure 6 of ref 19). We believe that the decrease in carbonate–carbonate  $^{13}\text{C}$ – $^{13}\text{C}$  coupling for interfacial relative to bulk polycarbonate (Figure 10) could be the result of a splaying of these carbonate moieties under the influence of the proximate fluorinated ring.

Although the REDOR dephasing for the polycarbonate–polyfluorostyrene blends indicates tight packing with no gaps at the interface, the DRSE results show no excess in packing density over that of bulk polycarbonate. On the other hand, recent experiments<sup>30</sup> involving dynamic nuclear polarization (DNP) electron-to-proton and electron-to-carbon magnetization transfers from free-radical doped polystyrene in one phase of a heterogeneous blend to  $^{13}\text{C}$ -labeled polycarbonate in the other showed inhibition of phenylene ring motion. These DNP results suggested an increase in polycarbonate chain packing at the interface, where the interface thickness was defined in terms of the range of the electron–proton and electron–carbon dipolar coupling. This definition means an interface in the DNP experiments with several times the thickness of the interface in the  $^{13}\text{C}$ – $^{19}\text{F}$  REDOR experiments. Assuming no qualitative difference in the structure of the interface formed by polystyrene and polyfluorostyrene with polycarbonate, a combination of results from the two types of experiments suggests that the density of polycarbonate chain packing is normal in the first and second layers nearest the interface, but then increases in the next few layers. This increase in density need only be a few percent to be effective in blocking ring flips.<sup>31,32</sup>

**Acknowledgment.** This work was supported by the Office of Naval Research.

## References and Notes

- (1) Utracki, L. A. *Polymer Alloys and Blends: Thermodynamics and Rheology*; Oxford University Press: New York, 1990; p 118.
- (2) Paul, D. R. *Adv. Chem.* **1996**, 211, 3.
- (3) Manson, J. A.; Sperling, L. H. *Polymer Blends and Composites*; Plenum Press: New York, 1976; p 109.
- (4) Wignall, G. D. In *Encyclopedia of Polymer Science and Engineering*; John Wiley & Sons: New York, 1987; p 112.
- (5) McBrierty, V. J.; Packer, K. J. *Nuclear Magnetic Resonance in Solid Polymers*; Cambridge University Press: Cambridge, 1993; p 213.
- (6) Gullion, T.; Schaefer, J. *Adv. Magn. Reson.* **1989**, 13, 55.
- (7) Schmidt, A.; Kowalewski, T.; Schaefer, J. *Macromolecules* **1993**, 26, 1729.
- (8) McKay, R. A. U.S. Patent 4,446,431, May 1, 1984.
- (9) Holl, S. M.; McKay, R. A.; Gullion, T.; Schaefer, J. *Macromolecules* **1990**, 90, 620.
- (10) Stejskal, E. O.; Schaefer, J.; Waugh, J. S. *J. Magn. Reson.* **1977**, 28, 105.
- (11) Gullion, T.; Baker, D. B.; Conradi, M. S. *J. Magn. Reson.* **1990**, 89, 479.
- (12) Tycko, R.; Dabbagh, G. *Chem. Phys. Lett.* **1990**, 173, 461.
- (13) Klug, C. A.; Zhu, W.; Merritt, M. E.; Schaefer, J. *J. Magn. Reson.* **1994**, 109, 134.
- (14) Bork, V.; Gullion, T.; Hing, A.; Schaefer, J. *J. Magn. Reson.* **1990**, 88, 523.
- (15) Rhim, W. K.; Elleman, D. D.; Vaughan, R. W. *J. Chem. Phys.* **1973**, 59, 3740.
- (16) Schaefer, J.; Stejskal, E. O.; McKay, R. A.; Dixon, W. T. *Macromolecules* **1984**, 17, 1479.
- (17) Schaefer, J.; Stejskal, E. O.; Garbow, J. R.; McKay, R. A. *J. Magn. Reson.* **1984**, 59, 150.
- (18) Merritt, M. E.; Christensen, A. M.; Kramer, K. J.; Hopkins, T. L.; Schaefer, J. *J. Am. Chem. Soc.* **1996**, 118, 11278.

- (19) Klug, C. A.; Zhu, W.; Tasaki, K.; Schaefer, J. *Macromolecules* **1997**, *30*, 1734.
- (20) Kowalewski, T.; Schaefer, J. *Polym. Mater. Sci. Eng.* **1997**, *76*, 215 (San Francisco ACS Meeting).
- (21) Whitney, D.; Yaris, R. *Macromolecules* **1997**, *30*, 1741.
- (22) McDowell, L. M.; Klug, C. A.; Beusen, D. D.; Schaefer, J. *Biochemistry* **1996**, *35*, 5395.
- (23) Goetz, J. M.; Schaefer, J. *J. Magn. Reson.* **1997**, *127*, 147.
- (24) Wang, P. K.; Slichter, C. P.; Sinfelt, J. H. *Phys. Rev. Lett.* **1984**, *53*, 82.
- (25) Henrichs, P. M.; Linder, M.; Hewitt, J. M.; Massa, D.; Isacson, H. V. *Macromolecules* **1984**, *17*, 2412.
- (26) Lee, P. L.; Schaefer, J. *Macromolecules* **1995**, *28*, 2577.
- (27) Inglefield, P. T.; Amici, R. M.; Hung, C.-C.; O'Gara, J. F.; Jones, A. A. *Macromolecules* **1983**, *16*, 1552.
- (28) Spiess, H. W. *Colloid Polym. Sci.* **1983**, *261*, 193.
- (29) Tong, G.; Pan, Y.; Dong, H.; Pryor, R.; Wilson, G. E.; Schaefer, J. *Biochemistry* **1997**, *36*, 9859.
- (30) Afeworki, M.; McKay, R. A.; Schaefer, J. *Macromolecules* **1992**, *25*, 4084.
- (31) Walton, J. H.; Lizak, M. J.; Conradi, M. S.; Gullion, T.; Schaefer, J. *Macromolecules* **1990**, *23*, 416.
- (32) Hansen, M. T.; Boeffel, C.; Spiess, H. W. *Colloid Polym. Sci.* **1993**, *271*, 446.

MA970629V